Preclinical assessment of ^{18}F-LW223; a novel TSPO radiotracer for the detection of inflammation using PET

Mark G. MacAskill[1,2], Tashfeen Walton[1,2], Lewis Williams[3], Timaeus Morgan[3], Carlos J. Alcaide-Corral[1,2], Agne Stadulyte[1,2], Chris-Anne McKenzie[4], Alastair Moss[1], Ralph BouHaidar[5], Rustam Al-Shahi Salman[6], Marc R. Dweck[1], Gillian A. Gray[1], David E. Newby[1], Christophe Lucatelli[2], Andrew Sutherland[3], Sally L. Pimlott[7,8], Adriana A.S. Tavares[1, 3]

1. University/ BHF Centre for Cardiovascular Science, University of Edinburgh, Edinburgh, UK. 2. Edinburgh Imaging, University of Edinburgh, Edinburgh, UK. 3. School of Chemistry, University of Glasgow, UK. 4. MRC Edinburgh Brain Tissue Bank, University of Edinburgh, UK. 5. Forensic Pathology, University of Edinburgh, UK. 6. Centre for Clinical Brain Sciences, University of Edinburgh, UK. 7. School of Medicine, University of Glasgow, UK. 8. NHS Greater Glasgow and Clyde, UK.

Introduction

- Upregulation of TSPO occurs during inflammation, most widely studied in neuroinflammation, but also in cardiovascular disease.
- The most vastly studied TSPO radiotracer is [^{11}C]-PK11195; however, it is limited by:
  - Short half-life isotope
  - High non-specific binding in vivo
- To date, the use of 2nd generation radiotracers have been complicated by inter-individual differences in binding affinity. <u>This is dependant on the rs6971 genetic polymorphism[1], unlike PK11195 which is unaffected.</u>
- From a library of compounds based on the structure of PK11195, we have developed ^{18}F-LW223 which is the first TSPO targeted ^{18}F-ligand not susceptible to the genetic polymorphism.

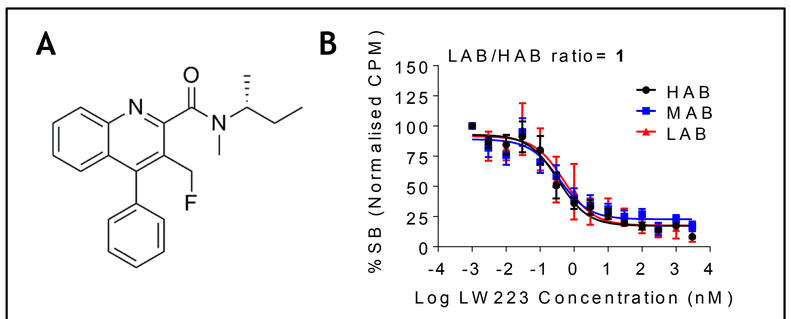

***Figure 1**. The structure of A)^{18}F-LW223 and **B)** its insensitivity to the rs6971 genetic polymorphism.*

Aims

The aims of this study were to:

1. **Assess the *in vivo* characteristics of ^{18}F-LW223 and its suitability for clinical translation.**
2. **Evaluate the ability of ^{18}F-LW223 to target human neuro/cardiovascular inflammation.**

Methods

<u>**PET Imaging Studies:**</u>

- Adult male Sprague-Dawley rats were used for all experiments, apart from dosimetry studies where mice were used.
- ^{18}F-LW223 distribution, kinetics and dosimetry were assessed using dynamic PET imaging.
- Radiotracer kinetics in the blood was assessed by automatic blood sampling.
- Radiometabolite studies were carried out using arterial blood samples and analysed by High Performance Liquid Chromatography (HPLC).
- Blocking experiments were carried out following administration of PK11195 (1mg/kg).

<u>***Ex-Vivo* Human ^{18}F-LW223 Binding:**</u>

- Diseased coronary vessels were obtained from sudden cardiac death patients.
- Brain tissue was obtained from subjects which had suffered a haemorrhagic stroke.
- Sections were exposed to ^{18}F-LW223 for 1 hour at room temperature, and imaging plates developed.

Results: ^{18}F-LW223 selectively targets TSPO

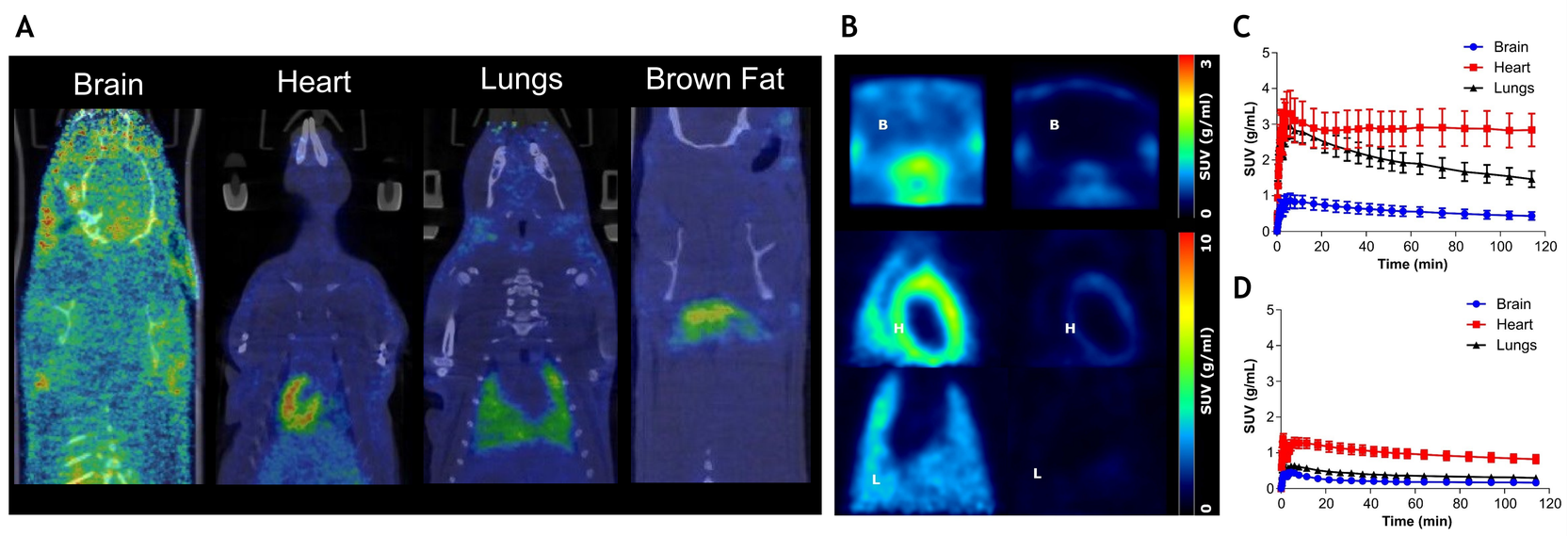

***Figure 2**. A) The in vivo distribution of ^{18}F-LW223. **B)** SUV sum images of ^{18}F-LW223 uptake before and after administered of PK11195 (1 mg/kg). **C)** Time activity curves for the major source organs at baseline and D) following PK11195 blockade. Results represent the mean ±SEM, n=3. Legend: B=brain, H=heart and L=lungs.*

Results: ^{18}F-LW223 is slowly metabolised and has a safe dosimetric profile

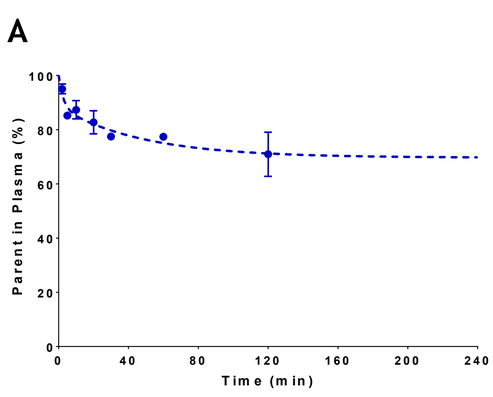

B

% Parent Fraction			
Organ	Time		
	15 min	60 min	120 min
Heart	95.21	91.79	92.01
Brain	100	100	87.29
Lungs	94.93	89.87	90.69
Spleen	95.21	91.91	89.93

C

Estimated Absorbed Dose (mGy/MBq)		
Target Organ	Male	Female
Adrenals	3.72E-02	4.38E-02
Brain	7.01E-03	8.38E-03
Breasts	9.21E-03	1.16E-02
Gallbladder Wall	2.42E-02	2.80E-02
LLI Wall	1.28E-02	1.61E-02
Small Intestine	3.38E-02	3.97E-02
Stomach Wall	1.23E-02	1.54E-02
ULI Wall	1.52E-02	1.89E-02
Heart Wall	3.07E-02	3.96E-02
Kidneys	2.38E-02	2.67E-02
Liver	1.56E-02	2.04E-02
Lungs	3.57E-02	4.52E-02
Muscle	1.02E-02	1.27E-02
Ovaries	1.40E-02	1.71E-02
Pancreas	1.35E-02	1.68E-02
Red Marrow	1.02E-02	1.25E-02
Osteogenic Cells	1.54E-02	2.01E-02
Skin	7.82E-03	9.71E-03
Spleen	1.19E-02	1.51E-02
Testes	9.46E-03	-
Thymus	1.16E-02	1.47E-02
Thyroid	1.02E-02	1.19E-02
Urinary Bladder Wall	1.37E-02	1.51E-02
Uterus	-	1.67E-02
Total Body	1.12E-02	1.40E-02
Effective Dose (mSv/MBq)	**1.53E-02**	**1.84E-02**

***Figure 3**. A) Blood kinetics of ^{18}F-LW223 showing the % parent fraction within plasma. **B)** % Parent fraction within organs. Results represent the mean ±SEM, n=3. **C)** Radiation absorbed dose estimates, LLI= lower large intestine, ULI= upper large intestine.*

Results: ^{18}F-LW223 selectively binds to inflammatory tissue

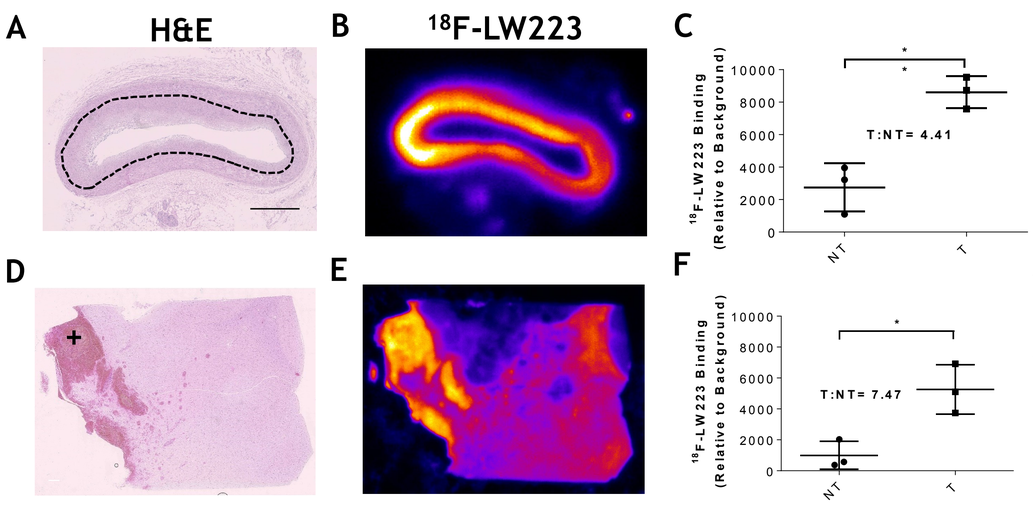

***Figure 4**. A) H&E staining of diseased coronary vessel with neointimal remodeling (dotted line) correlating with **B)** ^{18}F-LW223 binding. **C)** Target (T) to Non-Target (NT) ratios of ^{18}F-LW223 in diseased vessel. **D)** H&E staining of hemorrhagic stoke tissue (+) correlating with **E)** ^{18}F-LW223 binding. **F)** T:NT of ^{18}F-LW223 in stoke tissue. Results represent the mean ±SEM, n=3, *=p<0.05, **=p<0.01 using unpaired t test.*

Conclusions

- We have demonstrated that ^{18}F-LW223 selectively binds to TSPO *in vivo*, has a favourable kinetic profile, slow metabolism and safe dosimetric profile.
  - **<u>These findings support further clinical translation</u>**
- Additionally, our promising *ex-vivo* human binding results warrant further preclinical study of ^{18}F-LW223 in models of neurological and cardiovascular disease.

References

1. Owen, D. R. et al. J. Cereb. Blood Flow Metab. 32, 1–5 (2012).

Acknowledgements

The authors would like to thank the BHF and SINAPSE for supporting this work.